J Mater Sci: Mater Med (2010) 21:1881–1890
DOI 10.1007/s10856-010-4049-x

The pH-induced thermosensitive poly (NIPAAm-*co*-AAc-*co*-HEMA)-*g*-PCL micelles used as a drug carrier

Weifeng Dai · Yan Zhang · Zhengzhen Du · Minliang Ru · Meidong Lang

Received: 21 December 2009 / Accepted: 1 March 2010 / Published online: 10 March 2010

Abstract The macromonomer of 2-hydroxyethyl methyacrylate-caprolactone (HPCL) was synthesized by the ring-opening polymerization (ROP) of ε-caprolactone, which was initiated by 2-hydroxyethyl methyacrylate (HEMA). Then, the graft terpolymers of NIPAAm-*co*-AAc-*co*-HEMA-*g*-PCL (PHNA-CL) with varying mole ratios were subsequently synthesized by free radical polymerization of HEMA-PCL, *N*-isopropylacrylamide (NIPAAm) and acrylic acid (AAc). PHNA-CL was further self-assembled in different types of solvent. All the as-prepared copolymers were characterized by ^{1}H NMR, FT-IR and GPC. Micellization behaviors of micelles were studied by TEM and DLS. The micelles exhibited a phase transition temperature which can be readily adjusted by changing pH value of the micellization system. Micelle loaded with doxorubicin (DOX) was used to evaluate the drug release behavior. The release of DOX from micelles could be controlled by changing pH value and temperature in buffer solutions. The micelles are potentially to be used as a new anticancer drug carrier for intracellular delivery.

1 Introduction

In the past decade, nanospheres have presented a promising approach to decrease uptakes of drugs in reticuloendothelial system, especially liver and spleen after intravenous injection [1–5]. Amphiphilic block or graft copolymers composed of both hydrophilic and hydrophobic segments can form a micellar structure in a selected solvent, which can thermodynamically favor for one block, but unfavorable for the others [6–11]. The inner core is formed by hydrophobic segments, while the swollen shell is formed by hydrophilic segments. Therefore, the hydrophobic drugs could be easily incorporated into the core of micelles by either a covalent or a non-covalent bonding through hydrophobic interactions in aqueous media [12–14].

More recently, intelligent nanoparticles have attracted many interests in biomedical applications. Many distinctive intelligent nanoparticles, such as temperature, pH and light responsive nanoparticles, have been investigated in drug delivery system [15]. Among the stimuli sensitive polymers, poly(*N*-isopropylacrylamide) (PNIPAAm) and relative copolymers are widely investigated. PNIPAAm is a water-soluble polymer, which exhibits an extended chain conformation below the low critical solution temperature (LCST). The LCST of PNIPAAm in aqueous environment is around 32°C and is dependent on its molecular weight and molecular incorporation [16–20]. Therefore, the PNIPAAm copolymers have been widely studied as temperature sensitive polymeric nanoparticles. Also, pH-sensitive polymeric carriers have been developed for therapying targeted tumor, which basing on the mildly acidic pH embraced in tumor and inflammatory compartments of cells (pH ~6.8) as well as in the endosomal and lysosomal of cells (pH ~5–6). Furthermore, there has been considerable interest in developing nanoparticles (NPs) that responds to two stimuli [21, 22]. Based on this, some pH/temperature responsive hydrophiphilic segments have been prepared by copolymerizing NIPAAm with monomers containing an ionizable group, such as acrylic acid (AAc), to give pH dependent temperature response.

W. Dai · Y. Zhang · Z. Du · M. Ru · M. Lang (✉)
Key Laboratory for Ultrafine Materials of Ministry of Education, School of Materials Science and Engineering, East China University of Science and Technology, P.O. Box 391, 130 Meilong Road, 200237 Shanghai, People's Republic of China
e-mail: mdlang@ecust.edu.cn

Biodegradable polyesters, such as poly(ε-caprolactone) (PCL) and polylactides (PLA), have been extensively studied as carriers for controlled drug release. They are biocompatible, biodegradable and drug permeable, which are excellent choice for hydrophobic segment. Different polymeric NPs, like poly(enthyl glycol)-*b*-PCL micelles [23], poly(L-lactic acid)-*b*-poly(ethylene)-*b*-poly(L-histidine) micells [24], and PNIPAAm-*b*-PCL micells [25] have been designed by scientists in the past years. However, few core–shell nanoparticles assembled from graft copolymers have been developed. Core–shell nanoparticles which assembled from graft copolymers were less easy to prepare. This is due to the graft copolymers had less mobility and possible entangles. Hence, it may cause the hydrophobic cores to be exposed [26]. However, graft copolymers consist of several hydrophobic segments on a hydrophilic polymeric backbone offer the NPs with versatile properties, which draw scientists' attentions.

Doxorubicin (DOX) is known as a typical anti-tumor drug which is widely used in cancer chemotherapy. Unfortunately, DOX is also toxic to ordinary tissue. To avoid the acute toxicity of DOX, polymeric micelles have been designed as carriers of hydrophobic drugs [27, 28]. In this study, we successfully demonstrated a new route to design the micelle system which can be effectively used to control the DOX release. Namely, the random graft terpolymers PHNA-CLs with varying mole ratios were subsequently synthesized by free radical polymerization of HPCL, *N*-isopropylacrylamide (NIPAAm) and acrylic acid (AAc). When the pH is raised above the pKa of the acid groups, the shell of NPs consisting of NIPAAm and AAc exhibits an adjustable LCST [20]. More significantly, micelles formed with this type of copolymers were found to be an efficient carrier of DOX. Via reducing pH or increasing temperature, Poly(NIPAAm-*co*-AAc-*co*-HEMA) will collapse and the formed aggregation in outer shells may cause structural deformation of NPs' inner cores, namely DOX release was controlled.

2 Experimental section

2.1 Materials

N-isopropylacrylamide (NIPAAm) was purchased from Shanghai Wujing Chemical Reagent, China and recrystallized in cyclohexane before used. 2-hydroxyethyl methyacrylate (HEMA), ε-caprolactone (ε-CL) were obtained from Acros Oganic, USA and used after distillation under reduced pressure. Acrylic acid, 1,4-Dioxane, *N*,*N*′-Azobisisobutyronitrile (AIBN) and Dimethylformamide (DMF) were provided by Shanghai Chemical Reagent, China and used before distillation or recrystallization. DOX was obtained from Zhongshang Hospital. All other solvents were used as received from Shanghai Chemical Reagent, China.

2.2 Synthesis of graft copolymer

The ring-opening polymerization of 4.56 g (40 mmol) ε-caprolactone was carried out in the polymerization tube initiated by 0.130 g (1 mmol) HEMA using stannous octanoate as the catalyst (catalyst/monomer = 1 wt‰). Exhausting-refilling with dry argon repeatedly for three times, then the polymerization tube was sealed in vacuum and placed in an oil bath at 110°C for 24 h. After cooling to room temperature, the resulting product was dissolved in $CHCl_3$. The solution was added dropwise into the excess methanol to precipitate. The obtained macromonomer HEMA-PCL was dried in vacuum at room temperature until constant weight. The molecular weight of HEMA-PCL is 4600 Da, which is calculated by the signals intensity of I_j and I_b in Fig. 1a. By GPC analysis, the molecular weight is 5000 Da, closing to the analysis tested by ^{1}H NMR.

PHNA-CLs were synthesized by radical polymerization [20]. The NIPAAm/HEMA/AAc ratios were shown in Table 1. The total monomer concentration was 0.1 g/ml in 1,4-dioxane. AIBN was used as an initiator (initiator/total amount of monomer = 0.7 mol%). At room temperature, nitrogen was bubbled into the solution for 30 min prior to the addition of the initiator. The copolymerization was conducted at 65°C for 24 h in the nitrogen atmosphere. Excessive solvent was distilled under reduced pressure. Then, the solution was precipitated in an excess of diethyl ether. The precipitates were isolated by filtration and dried in a vacuum oven at room temperature until constant weight.

2.3 Characterizations of copolymers

All synthetic process of copolymers was illustrated in Scheme 1 and was listed in Table 1. The compositions of copolymers were calculated by ^{1}H NMR spectra and acid titration. Briefly, 0.1 g PHNA-CL was dissolved in 20 ml dichloromethane, then it's titrated by 0.01 N NaOH dissolved in ethanol using phenolphthalein as an indicator. The amount of AAc in the copolymer calculated from the amount of NaOH required for neutralization. All the samples were tested in triplicate. Then, the mole composition of the copolymer was calculated by Eq. 1:

$$\begin{aligned} &F_{HPCL} + F_{NIPAAm} + F_{AAC} = 1; \\ &F_{HPCL}/F_{NIPAAm} = I_m/3I_f \quad F_{AAC} = w_{AAC}/72 \end{aligned} \tag{1}$$

where w_{AAC} is the mass ratio of AAc and the relative intensity is the appropriate resonance of ^{1}H NMR spectra.

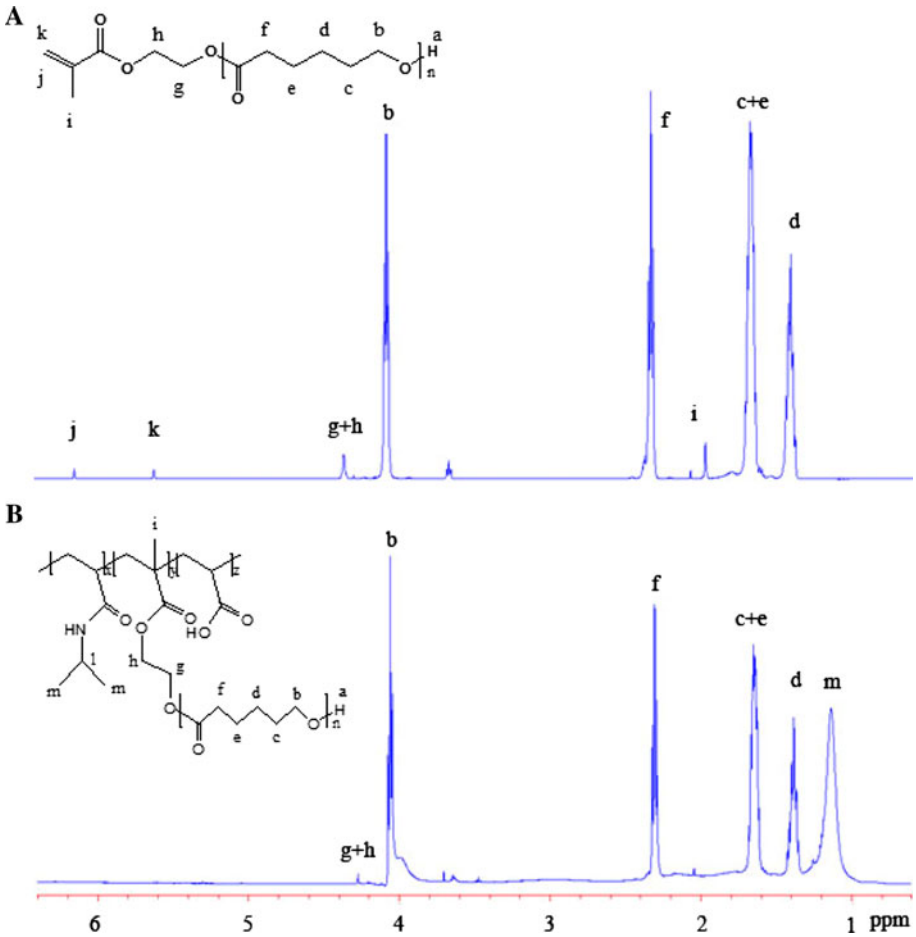

Fig. 1 ^{1}H NMR spectra of macromonomer (**a**) and random graft terpolymer (**b**) in $CDCl_3$

Table 1 Characterization of terpolymers with different feed ratio

Terpolymer	In feed (x)[a]			In terpolymer (x)[a]			Yield (%)	Mn[c] $\times 10^4$	PDI[d]
	HPCL	NIPAAm	AAc	HPCL[b]	NIPAAm[b]	AAc[b]			
PHNA-CL-A	1.0	90.0	9.0	1.8	87.8	10.4	84	5.25	1.96
PHNA-CL-B	2.0	89.0	9.0	3.1	86.9	10.0	83	4.51	2.43
PHNA-CL–C	3.0	88.0	9.0	4.5	82.8	12.7	84	4.72	1.60
PHNA-CL-D	1.0	87.5	11.5	2.3	83.7	13.0	76	6.24	1.90
PHNA-CL-E	1.0	82.5	16.5	2.5	76.1	21.4	90	4.28	2.03

[a] x is the molar ratio of HPCL, NIPAAm and AAc

[b] Molar ratio of HPCL, NIPAAm and AAc was analyzed from ^{1}H NMR and titration

[c] Molecular weight was determined by GPC in THF using polystyrene as calibration standard

[d] PDI is polydispersity index which measured by GPC

The mole fraction of the monomers in the copolymers fits the feed, consistent with the sufficient conversion.

2.4 Preparation of polymer micelle and DOX loading to micelles

Pre-dissolved PHNA-CL (15 mg), in 5 ml DMF was dropwise added into 10 ml distilled water under stirring. Thereafter, the mixture was dialyzed against deionized water for 48 h at room temperature using cellulose membrane bag (MWCO = 14,000 Da, purchased from Shanghai Green Bird Science & Technology Development Co., LTD, China). The distilled water was replaced every 4 h. Then, NPs supernatant was frozen and lyophilized by freeze dryer system to obtain dried NPs products.

DOX was deprotonated at pH 9.6 to obtain the hydrophobic DOX and dried in a vacuum under room temperature. Then 15 mg of copolymer and 4 mg of DOX was

Scheme 1 The synthetic route of the NIPAAm-*co*-AAc-*co*-HEMA-*g*-PCL

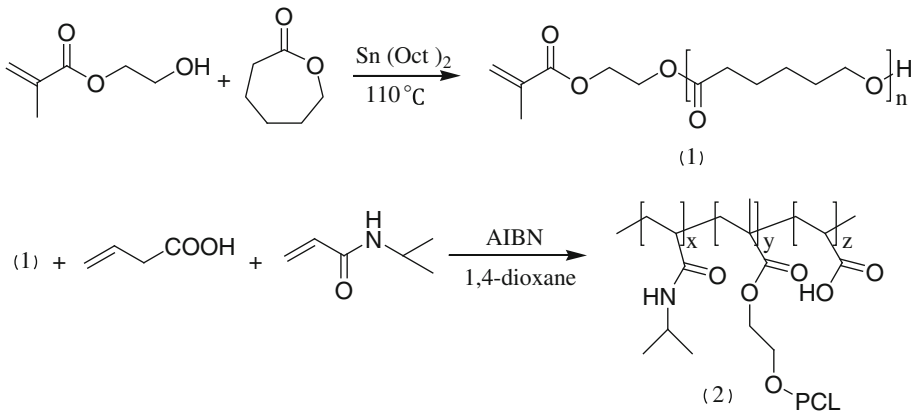

dissolved in 5 ml DMF. Applying the same procedure, DOX-loaded micelles were formed. To remove free DOX, the micelles was purified by filtered the mixture solution through a Millipore Millex-HV (Hydrophilic PVDF 0.45 μm).

3 Characterization of nanoparticles

3.1 Fluorescence spectroscopy

Aliquots of pyrene solutions (1.54×10^{-5} M in acetone, 400 μl) were added to 10 ml volumetric flasks respectively, and acetone was evaporated. Polymer solutions with concentrations ranged from 1.0×10^{-7} to 1.0 g/l were prepared in phosphate buffer solution (pH = 7.4). 10 ml of aqueous solution was then added to the volumetric flasks containing the pyrene residue. The change of the intensity ratio (I_{338}/I_{333}) of the pyrene with polymer concentration was plotted, while excitation spectra from 280 to 450 nm and emission wavelength at 390 nm. The critical micelle concentration (CMC) at pH 7.4 was determined by cross-over point at low polymer concentration in the plot.

3.2 pH-dependent phase transition determination

The cloud point measurement (turbidimetry) method was employed to measure LCST of micelles,. Briefly, the micelles were dispersed in different pH buffered solution (1 mg/ml, pH = 3.6, 4.6, 5.0, 7.4, ion strength I = 0.1 M). The optical transmittances of these solution were measured at 500 nm wavelength by UV–Vis spectrometer (Lambda 35, USA) with increasing solution temperature (20–50°C). The samples were stabilized 10 min while temperature raised every 3°C. Values for the LCST of samples were determined at a temperature with a half of the optical transmittance.

3.3 Dynamic light-scattering measurement

The particle size and size distribution of the thermosensitive micelles were investigated by dynamic light scattering (Autosizer 4700, Malvern), which was equipped with an argon laser operator at 532 nm with a fixed scattering angle of 90°. Before measurement, the NPs were sonicated for 1 min, and filtered through a 0.45 μm pore size filter to remove large aggregates.

3.4 Transmission electron microscopy measurements

Morphology of micelles was studied by a transmission electron microscopy (TEM) (Hitachi H-600). The samples were prepared by dropping diluted sphere suspensions containing 1.5% phosphotungstic acid (PTA, negative staining) onto the copper grids coated with a thin polymer film and then dried in a 30°C vacuum.

3.5 Drug loading efficiency and encapsulation

To investigate the efficacy of the NPs as drug carrier, hydrophobic DOX was loaded into the NPs and drug release patterns were studied. To measure drug content, drug loaded NPs were dissolved in DMF (0.2 mg/ml). The solution was sonicated for 5 min, and was taken for measurement of drug concentration by using a UV–Vis spectrophotometer at 485 nm. The drug loading efficiency (DLE) and drug entrapment efficiency (DEE) were calculated as following formulas:

$$\mathrm{DLE} = \frac{\text{amount of drug in micelles}}{\text{amount of drug} - \text{loaded micelles}} \times 100\% \qquad (2)$$

$$\mathrm{DEE} = \frac{\text{amount of drug in micelles}}{\text{amount of drug fed}} \times 100\% \qquad (3)$$

3.6 Drug release assay

The release behaviors of micelles loaded with DOX were studied in different pH values buffer solutions and different temperatures in pH 7.4 buffer solutions respectively. Generally speaking, 5 mg of micelles loaded with DOX solution were dispersed in 5 ml buffer solution, and then transferred in a dialysis membrane tube (MWCO = 14,000, purchased from Shanghai Green Bird Science & Technology Development Co., LTD, China). This tube was immersed in a vial containing 100 ml of buffered solution. The drug release from micelles was tested with constant shaking (100 rpm) at a certain temperature. The outer phase of the tube was withdrawn 5 ml for test and renewed with equivalent fresh buffer solution. The measurement of DOX concentration was conducted by a UV–Vis spectrophotometer.

3.7 Other measurements

^{1}H NMR and ^{13}C NMR experiments were carried out on a Bruker nuclear magnetic resonance instrument at 500 and 125 MHz using $CDCl_3$ as solvent and tetramethylsilane as internal reference. FT-IR spectra were recorded on films or KBr pellets by Nicolet FT-IR spectrometer (Magna-IR 550). Size exclusion chromatography (SEC) measurements performed in THF as the eluent (1.0 ml/min) with a Water 2414 HPLC pump, three ultrastyragel columns (2×10^5, 1×10^5, and 5×10^4 Å) in series, and a refractive index detector.

4 Result and discussion

4.1 Characterizations of HPCL and PHNA-CL

The structures of HEMA-PCL and PHNA-CL were confirmed by NMR spectra. As demonstrated in Fig. 1a, the peaks at 4.11, 2.38, 1.62 and 1.22 ppm are the signals of PCL. The triplet signal at 3.62 ppm corresponds to the methylene protons of the $–CH_2–OH$ end groups of the PCL-HEMA. And the characteristic signals of the olefinic protons at the end of the chain can be pointed out at 6.11 and 5.60 ppm. The mole ratio of NIPAAm and PCL is calculated from the integration ratio between the methyl protons (6H) of NIPAAm at 1.12 ppm and methylene protons (2H) of PCL at 2.38 ppm which shown in Table 1. In Fig. 1b, the disappearance of the signals at 6.11 and 5.60 ppm indicates that the majority of the end double bonds of HEMA-PCL have been converted into carbon–carbon single bonds to form the main chain during radical polymerization [29].

Figure 2 illustrates the ^{13}C NMR spectra of HEMA-PCL and PHNA-CL. In Fig. 2a, the olefins groups' peaks at 121.5 and 132.1 ppm confirm the introducing of HEMA to the end of PCL. Furthermore, the presence of peak at 19.1 ppm is the characteristic peak of CH_3. The appearance of peaks at 62.3 and 62.8 ppm are the characteristic peaks of methylene groups of HEMA. The peak at 23.3 ppm of Fig. 2b corresponds to the methyl groups of NIPAAm. In addition, the peaks at 43.2 ppm of –C–C– groups and at 174.5 ppm of C=O groups also clearly demonstrate the copolymerization of HEMA-PCL with NIPPAAm and AAc. All the evidences proved a graft polymer was synthesized successfully.

4.2 Analysis of nanoparticles

As mentioned by Riess [30] the critical micelle concentration (CMC) could be determined by fluorescence spectrophotometer. Figure 3 shows excitation spectrum of pyrene in the presence of the grafted polymers with a series of concentrations [31]. The CMC value of the graft copolymer was determined by the standard fluorescence spectroscopic [32].

Figure 4 plots show the intensity ratio of I_{338}/I_{333} from pyrene excitation spectra versus log C for PHNA-CL-A. Below the CMC, there are no micelles present in the solution. At the CMC, the micelles form and pyrene preferentially solubilize into the interior of the hydrophobic micelle cores. Thus, the fluorescence intensity is affected by the change of the copolymer concentration. From Table 2, it is observed that CMC values decreased while the content of ε-CL increased. It was reported the onset of micellization was determined mainly by the nature and length of the hydrophobic block [23], which was also confirmed in the graft copolymer. However, under a certain content of ε-CL, the CMC decreased with increasing content of AAc, which may attribute to the increasing of hydrophilicity in backbone chain.

The size of particle is dominated by the hydrophobic block. As shown in Table 2, the size of micelles increased with the increasing content of ε-CL. DOX-loading cause obvious size increases for PHNA-CL-A, PHNA-CL-B and PHNA-CL-C micelles while PHNA-CL-D and PHNA-CL-E with minor increases. Similar results were also obtained by other researchers [33]. Figure 5 is the size distribution of DOX-free (a) and DOX-loaded (b) micelles based on PHNA-CL-A. It is obvious that both the size and (distribution) of DOX-loaded micelles increase faster than that of DOX-free, which could be further demonstrated by the TEM image. Besides that, Figs. 5 and 6 show that self-assembled micelles were well dispersed and had regular spherical shapes with a narrow distribution.

Highly molecular weight PAAc is a well-known bioadhesive polymer. Random copolymers of AAc and PNIPAAm will lose the temperature sensitivity when the

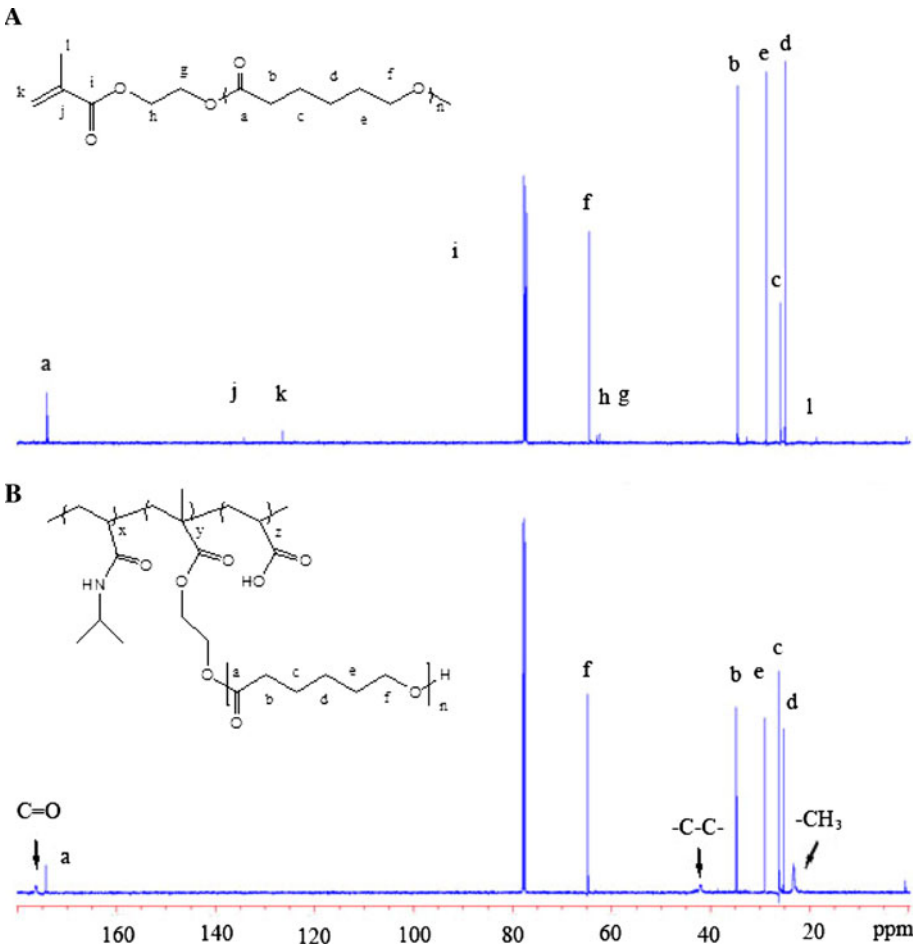

Fig. 2 ^{13}C NMR spectra of macromonomer (**a**) and random graft terpolymers (**b**) in $CDCl_3$

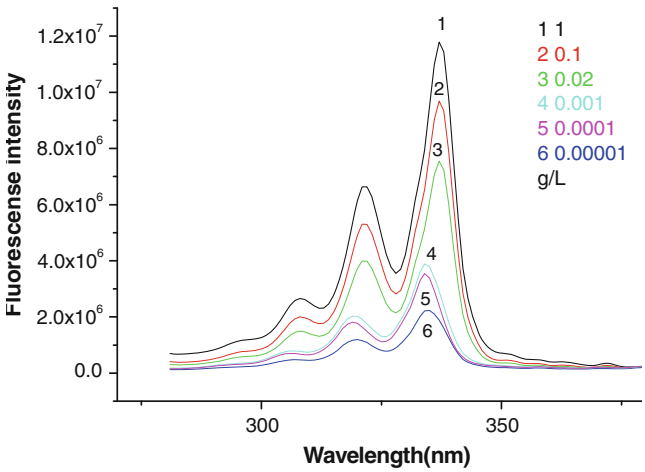

Fig. 3 The fluorescence excitation spectra of pyrene (6.0×10^{-7} M) as a function of PHNA-CL-A concentrations

content of the AAc increased to the point where the bio-adhesive properties are obtained. The core–shell nanoparticles self-assembled from the graft copolymers indeed showed a pH-dependent LCST. It is most likely triggered by the protonation and de-protonation of carboxylic acid groups in the hydrophilic segments of polymer, which is significantly affected by the molar ratio of NIPAAm and AAc.

Figure 7 and 8 are the graphs of absorbance versus temperature at a range of pH values, which are listed in Table 3. All of them show the LCST variations with different temperature and pH tested by cloud point experiments. However, the LCST is only observed at low pH value but absent at values above pH 5.0. It is considered that the graft copolymers exhibited a pH and temperature-induced phase transitions. It could be attributed to the formation of inter- and intra-molecular hydrogen bonding complexes between acid moieties of the amide groups and the amide groups of PNIPAAm. Above pH 5.0, no LCST was observed because the carboxylic acid groups are fully ionized for the exothermic water interaction of the carboxylic acid groups [34]. As shown in Fig. 7, the LCST of PHNA-CL-A increased with the increasing of pH values. At low pH value, the phase transition is rapid, while the transition curve is relaxed at pH 5.0. It is believed the competition of hydrogen bonding of PAAc/PNIPAAm and H_2O/PNIPAAm is the primary reason. Figure 8 is the plot of transmittance of random terpolymer solutions with different content of AAc. While increasing the content of

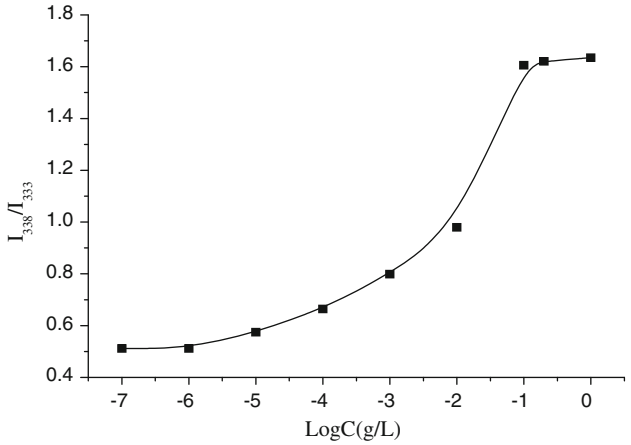

Fig. 4 Plots of I_{338}/I_{333} versus log C for PHNA-CL-A

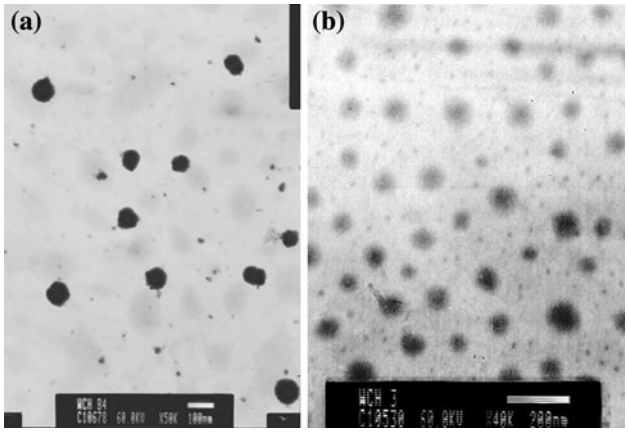

Fig. 6 TEMs of DOX-free (**a**) and DOX-loaded (**b**) micelles based on PHNA-CL-A

Table 2 Characterization of the micelles of random terpolymers

Sample	Particle size (nm)				CMC (mg/l)[b]
	DOX-free	PDI	DOX-loaded	PDI[a]	
PHNA-CL-A	79.8	0.190	117.5	0.292	0.794
PHNA-CL-B	102.5	0.201	128.0	0.242	0.570
PHNA-CL-C	113.6	0.302	129.3	0.311	0.486
PHNA-CL-D	91.1	0.192	97.6	0.220	1.52
PHNA-CL-E	98.9	0.187	101.2	0.201	2.00

[a] PDI is polydispersity index which measured by DLS

[b] CMC is determined by fluorescence spectrophotometer

AAc, the LCST increases and the phase transition relaxes. It is also worthy noted the content of PCL did not have significant effect on the LCST, which is shown in Fig. 9 and Table 3.

4.3 Drug loading and release studies

The thermosensitive PHNA-CL micelles were investigated as drug carriers for loading hydrophobic model drug of DOX. The amount of DOX was introduced into the micelles by controlling the weight ratio between polymer and drug is shown in Table 4. The drug/carrier ratio of 4/15 mg of different PHNA-CLs exhibits similar drug loading efficiency. Moreover, the PHNA-CL graft copolymers exhibit excellent drug entrapment efficiency (32.98–62.62%). The drug loading efficiencies and drug contents also show a general trend of increasing these efficacies with PCL content increment. Interestingly, increasing content of AAc also increase the efficiency of drug entrapment. It is recognized the carboxylic groups of hydrophilic segments strengthened the force between the shell and DOX. Beside that, different drug/carrier weight ratios of 2/15, 4/15 and 6/15 were also studied. The DLE increased with increasing DOX feeding content while DEE not changed regularly.

Figure 9 shows the DOX release from nanoparticles at different pH values. The PHNA-CL-A micelles exhibit a certain initial release rate in the solution. The initial burst effect was observed due to untrapped DOX released from the outer shell. The DOX loaded micelles exhibit sustained release of about 40–80% in the different pH values for 48 h and some drug has not been released for the strong hydrophobic interaction between PCL segments and DOX. The drug release from the micelles at pH 7.4 was considerably slow. On the contrary, the drug release was faster at pH 6.0 at 37°C, with 80% of the drug released within 48 h and about 62% at pH 6.8. DOX is well water soluble under

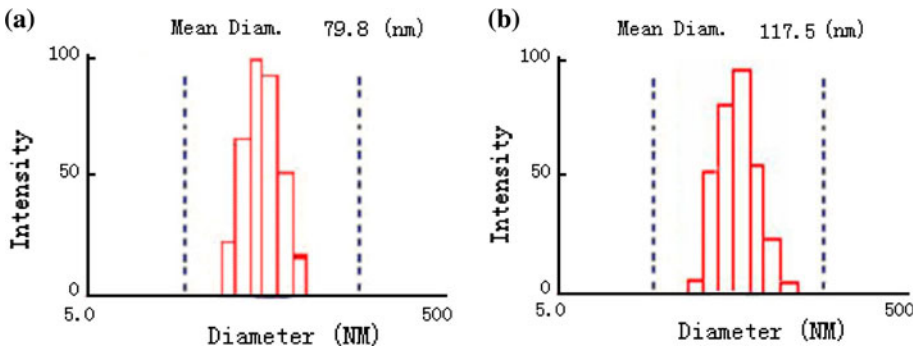

Fig. 5 Size distributions of DOX-free (**a**) and DOX-loaded (**b**) micelles based on PHNA-CL-A

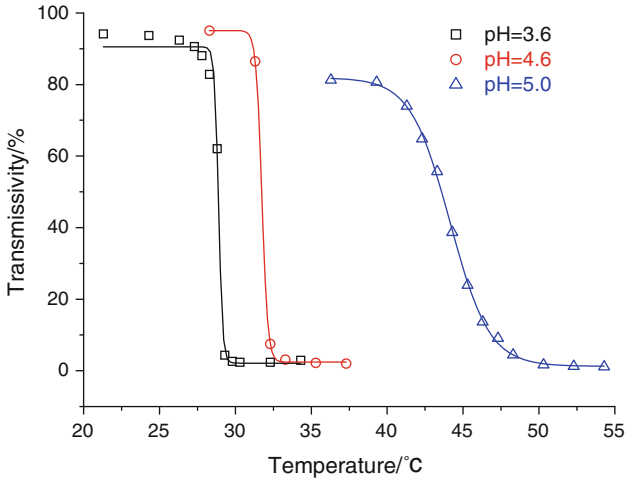

Fig. 7 Plot of transmittance of PHNA-CL-A solutions with different pH as a function of temperature at varying pH at 500 nm

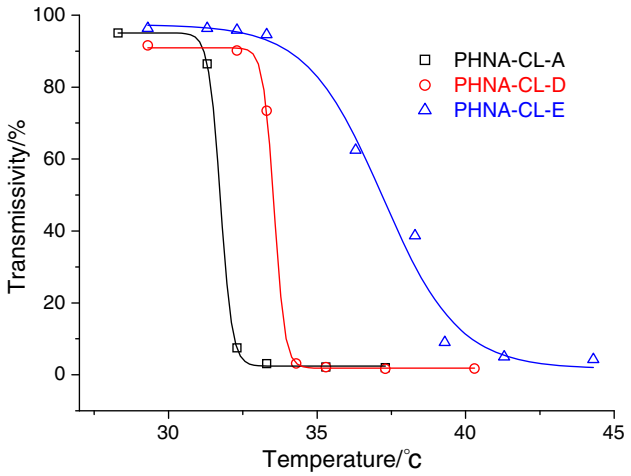

Fig. 8 Plot of transmittance of random terpolymer solutions with different content of AAc as a function of temperature pH = 4.6 at 500 nm

Table 3 LCST of the core–shell micelles of terpolymers at different pH values

Sample	pH = 3.6 (°C)	pH = 4.6 (°C)	pH = 5.0 (°C)	pH > 5.0
PHNA-CL-A	28.9	31.7	44.1	–
PHNA-CL-B	29.8	32.5	45.0	–
PHNA-CL-C	27.4	31.8	42.6	–
PHNA-CL-D	28.7	33.5	48.0	–
PHNA-CL-E	28.9	37.2	–	–

acidic environment because it is protonized more under acidic condition than under neutral conditions, so the partition coefficient is more shifted towards release from the hydrophobic micellar core at low pH [12, 35]. Also, the

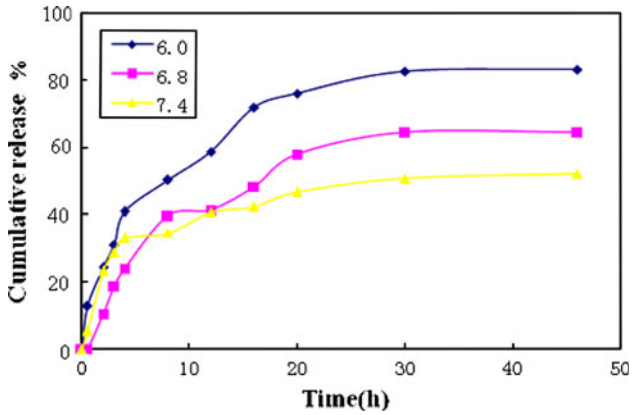

Fig. 9 Cumulative drug release of PHNA-CL-A micelles in the different pH solution at 37°C

Table 4 Drug-loading contents of copolymer nanoparticles with DOX

Sample	Copolymer (mg)	DOX (mg)	DLE (%)	DEE (%)
PHNA-CL-A	15	4	8.08	32.98
PHNA-CL-B	15	4	10.15	42.36
PHNA-CL-C	15	4	11.06	46.35
PHNA-CL-D	15	4	12.98	55.96
PHNA-CL-E-1	15	2	7.17	57.90
PHNA-CL-E-2	15	4	14.2	62.62
PHNA-CL-E-3	15	6	17.43	52.72

change in pH value may lead to the deformation and precipitation of the core–shell nanoparticles, thereby causing the release of the enclosed drug.

Figure 10 illustrates the DOX release behavior at different temperature. When the temperature is 32°C, the drug release is slow. While the temperature is 42°C, the drug release rate was appreciable increased. However, comparing with the change of pH values, the change of temperatures does not affect the release rate significantly. It is believed that the phase transition of PNIPAAm in the copolymer at pH 7.4 disappeared for the exothermic water interaction of the carboxylic acid groups competing with the entropic driving force of the phase separation of the PNIPAAm homopolymer. Only did the gently shrink of the shell of nanoparticles accelerated the drug release slightly.

5 Conclusion

Intelligent micelles with multi-functional sensitivities have been prepared by self-assembly of PHNA-CL. The micelles exhibit a temperature-induced phase transitions while pH value is no higher than 5.0, which were investigated as drug carrier by loading DOX. The drug release

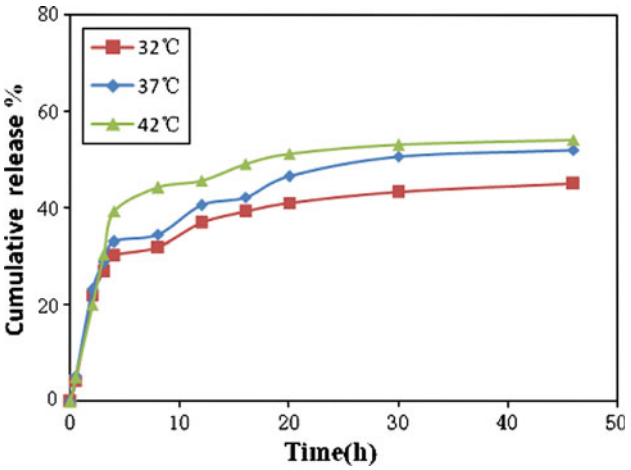

Fig. 10 Cumulative drug release of PHNA-CL-A micelles in the different pH 7.4 solution at different temperature

from the micelles at pH 7.4 (37°C) was considerably slow, while it is much faster at pH 6.0 and pH 6.8 respectively. Furthermore, the drug release at different temperature was also studied. Notably, the drug released faster at a higher temperature. Owe to the mildly acidic pH condition embraced in tumor, inflammatory compartments and an adjustable body temperature within limits, the intelligent micelles have great potential in intracellular drug delivery for cancer therapy.

Acknowledgments Financial support from National Natural Science Foundation of China (Nos. 20674019, 20804015), Natural Science Foundation of Shanghai (No. 08ZR1406000), Doctoral Fund of Ministry of Education of China (Nos. 20060251015, 200802511021), and Shanghai Leading Academic Discipline Project (B502) are gratefully acknowledged.

References

1. Letchford K, Liggins R, Burt H. Solubilization of hydrophobic drugs by methoxy poly(ethylene glycol)-*block*-polycaprolactone diblock copolymer micelles: theoretical and experimental data and correlations. J Pharm Sci. 2008;97:1179–90.
2. Yáñez JA, Forrest ML, Ohgami Y, Kwon GS, Davies NM. Pharmacometrics and delivery of novel nanoformulated PEG-b-poly(ε-caprolactone) micelles of rapamycin. Cancer Chemother Pharm. 2008;61:133–44.
3. Lin JP, Zhang SN, Chen T, Lin SL, Jin HT. Micelle formation and drug release behavior of polypeptide graft copolymer and its mixture with polypeptide block copolymer. Int J Pharm. 2007; 336:49–57.
4. Ko JY, Park K, Kim YS, Kim MS, Han JK, Kim K, et al. Tumoral acidic extracellular pH targeting of pH-responsive MPEG-poly(β-amino ester) block copolymer micelles for cancer therapy. J Control Release. 2007;123:109–15.
5. Soppimath KS, Liu LH, Seow WY, Liu SQ, Powell R, Chan P, et al. Multifunctional core/shell nanoparticles self-assembled from pH-induced thermosensitive polymers for targeted intracellular anticancer drug delivery. Adv Funct Mater. 2007;17:355–62.
6. Gao ZS, Eisenberg A. A model of micellization for block copolymers in solutions. Macromolecules. 1993;26:7353–60.
7. Tanodekaew S, Pannu R, Heatley F, Attwood D, Booth C. Association and surface properties of diblock copolymers of ethylene oxide and DL-lactide in aqueous solution. Macromol Chem Phys. 1997;198:927–44.
8. Kim SY, Shin ILG, Lee YM, Cho CS, Sung YK. Methoxy poly(ethylene glycol) and ε-caprolactone amphiphilic block copolymeric micelle containing indomethacin. II. Micelle formation and drug release behaviours. J Control Release. 1998;51:13–22.
9. Lee ALZ, Wang Y, Ye WH, Yoon HS, Chan SY, Yang YY. Efficient intracellular delivery of functional proteins using cationic polymer core/shell nanoparticles. Biomaterials. 2008;29:1224–32.
10. Mahmud A, Xiong XB, Lavasanifar A. Novel self-associating poly(ethylene oxide)-block-poly(ε-caprolactone) block copolymers with functional side groups on the polyester block for drug delivery. Macromolecules. 2006;39:9419–28.
11. Kim BS, Taton TA. Biocompatible polymer vesicles from biamphiphilic triblock copolymers and their interaction with bovine serum albumin. Langmuir. 2007;23:2224–30.
12. Nakanishi T, Fukushima S, Okamoto K, Suzuki M, Matsumura Y, Yokoyama M, et al. Development of the polymer micelle carrier system for doxorubicin. J Control Release. 2001;74:295–302.
13. Lee ES, Na K, Bae YH. Super pH-sensitive multifunctional polymeric micelle. Nano Lett. 2005;5:325–9.
14. Hrubý M, Koňák Č, Ulbrich K. Polymeric micellar pH-sensitive drug delivery system for doxorubicin. J Control Release. 2005; 103:137–48.
15. Rijcken CJF, Soga O, Hennink WE, Nostrum CFV. Triggered destabilisation of polymeric micelles and vesicles by changing polymers polarity: an attractive tool for drug delivery. J Control Release. 2007;120:131–48.
16. Chung JE, Yokoyama M, Okano T. Inner core segment design for drug delivery control of thermo-responsive polymeric micelles. J Control Release. 2000;65:93–103.
17. Hobabi MR, Hassanzadeh D, Azarmi S, Entezami AA. Effect of synthesis method and buffer composition on the LCST of a smart copolymer of *N*-isopropylacrylamide and acrylic acid. Polym Adv Technol. 2007;18:986–92.
18. Cheng C, Wei H, Shi BX, Cheng H, Li C, Gu ZW, et al. Biotinylated thermoresponsive micelle self-assembled from double-hydrophilic block copolymer for drug delivery and tumor target. Biomaterials. 2008;29:497–505.
19. Bikram M, Gobin AM, Whitmire RE, West JL. Temperature-sensitive hydrogels with SiO_2–Au nanoshells for controlled drug delivery. J Control Release. 2007;123:219–27.
20. Chen GH, Hoffman AS. Graft copolymers that exhibit temperature-induced phase transitions over a wide range of pH. Nature. 1995;373:49–52.
21. Lo CL, Lin KM, Hsiue GH. Preparation and characterization of intelligent core-shell nanoparticles based on poly(D, L-lactide)-g-poly(N-isopropyl acrylamide-co-methacrylic acid). J Control Release. 2005;104:477–88.
22. Soppimath KS, Tan DCW, Yang YY. pH-Triggered thermally responsive polymer core-shell nanoparticles for drug delivery. Adv Mater. 2005;17:318–23.
23. Shin ILG, Kim SY, Lee YM, Cho CS, Sung YK. Methoxy poly(ethylene glycol)/ε-caprolactone amphiphilic block copolymeric micelle containing indomethacin: I. Preparation and characterization. J Control Release. 1998;51:1–11.
24. Lee ES, Oh KT, Kim D, Youn YS, Bae YH. Tumor pH-responsive flower-like micelles of poly(L-lactic acid)-*b*-poly(ethylene glycol)-*b*-poly(L-histidine). J Control Release. 2007;123:19–26.
25. Choi CY, Chae SY, Nah JW. Thermosensitive poly(*N*-isopropylacrylamide) -*b*-poly(ε-caprolactone) nanoparticles for efficient drug delivery system. Polymer. 2006;47:4571–80.

26. Chung JE, Yokoyama M, Aoyagi T, Sakurai Y, Okano T. Effect of molecular architecture of hydrophobically modified poly (*N*-isopropylacrylamide) on the formation of thermoresponsive core-shell micellar drug carriers. J Control Release. 1998;53: 119–30.
27. Campbell RB, Balasubramanian SV, Straubinger RM. Influence of cationic lipids on the stability and membrane properties of paclitaxel-containing liposomes. J Pharm Sci. 2001;90:1091–105.
28. Sharma A, Mayhew E, Bolcsak L, Cavanaugh C, Harmon P, Janoff A, et al. Activity of paclitaxel liposome formulations against human ovarian tumor xenografts. Int J Cancer. 1997; 71:103–7.
29. Ru ML, Dai WF, Du ZZ, Lang MD. Synthesis and self-assembly behavior of random graft terpolymers. Acta Chimica Sinica. 2008;66:1884–8.
30. Riess G. Micellization of block copolymers. Prog Polym Sci. 2003;28:1107–70.
31. Liu XM, Pramoda KP, Yang YY, Chow SY, He CB. Cholesteryl-grafted functional amphiphilic poly(N-isopropylacrylamide-*co*-N-hydroxylmethylacrylamide): synthesis, temperature-sensitivity, self-assembly and encapsulation of a hydrophobic agent. Biomaterials. 2004;25:2619–28.
32. Tang DM, Lin JP, Lin SL, Zhang SN, Chen T. Self-assembly of poly(γ-benzyl L-glutamate)-*graft*-poly(ethylene glycol) and its mixtures with poly(γ-benzyl L-glutamate) homopolymer. Macromol Rapid Commun. 2004;25:1241–6.
33. Shuai XT, Ai H, Nasongkla N, Kim S, Gao JM. Micellar carriers based on block copolymers of poly(ε-caprolactone) and poly(ethylene glycol) for doxorubicin delivery. J Control Release. 2004;98:415–26.
34. Jones MS. Effect of pH on the lower critical solution temperatures of random copolymers of *N*-isopropylacrylamide and acrylic acid. Eur Polym J. 1999;35:795–801.
35. Kataoka K, Matsumoto T, Yokoyama M, Okano T, Sakurai Y, Fukushima S, et al. Doxorubicin-loaded poly(ethylene glycol)-poly(beta-benzyl-L-aspartate)copolymer micelles: their pharmaceutical characteristics and biological significance. J Control Release. 2000;64:143–53.